OCEANUM
OCEAN NUMERICAL

Technical Note on Specification and Validation of the Oceanum Global Wave Hindcast

July 2020

Model	WAVEWATCH III v6.07
Period	Jan 1979 - Dec 2019
Spatial resolution	0.5 degrees (~50km)
Temporal resolution	3 hourly
Region	0E-360E longitude
	77S-77N latitude
Forcings	ERA5 winds and ice

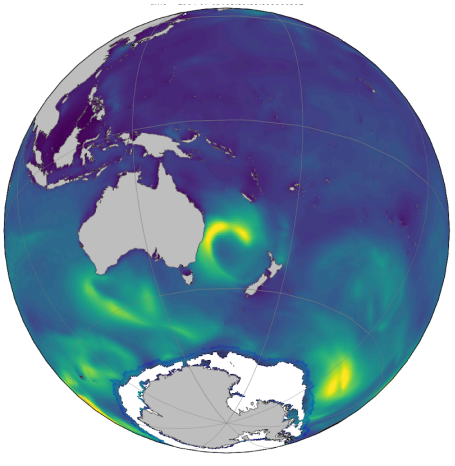

Introduction

Knowledge of historical wave conditions is necessary for many human endeavours, such as offshore structure design, coastal hazard assessment, and renewable energy applications to name a few. Studies of wave climate require datasets of sufficient duration and resolution, qualities that vary according to the specific application. Numerical wave models provide a valuable means of supplementing the sparse historical observation record.

Until recently, the quality of available wave hindcast data was relatively poor, which is primarily a reflection of the quality of the available reanalysis winds. The release of the Climate Forecast System Reanalysis (CFSR: Saha et al. 2010) heralded a step-change in resolution and accuracy, spurring a series of subsequent wave hindcasts (e.g. Chawla et al. 2012; Durrant et al. 2014; Rascle and Ardhuin 2013). This wind improvement coupled with advances in wave model physics (e.g. Ardhuin et al. 2010; Tolman et al. 2013; Zieger et al. 2015) resulted in a significant improvement in the quality of data available. The recently released ECMWF Reanalysis 5th Generation (ERA5) provides another such step change.

CFSR was known to suffer from inhomogeneities through time, due to changes in the assimilated observations, to which the waves are particularly sensitive (e.g Chawla et al. 2009). Most notably, a stepwise reduction in the upper percentile winds is noted around 1993, as well as an increase in the latter years of the hindcast which can be directly seen in the wave CFSR driven hindcasts (e.g. Chawla et al. 2012; Durrant et al. 2014; Rascle and Ardhuin 2013) reducing their efficacy in climate climate applications (e.g. Hemer et al. 2016). Overall, the issues associated with temporal consistency in CFSR is greatly improved with ERA5.

ERA5 is produced by the European Centre for Medium-Range Weather Forecasts (ECMWF). It uses the Integrated Forecast System (IFS) CY41R2 (ECMWF 2016), assimilating an unprecedented amount of historical observations using 4D var assimilation. The system is run with 137 hybrid sigma/pressure model levels in the vertical, with the top-level at 0.01 hPa. The IFS is coupled to a soil model and an ocean wave model. Winds and ice concentration data are available at a 31 km resolution at hourly intervals. ERA5 represents a significant upgrade from the previous ECMWF's reanalysis product, the ERA-Interim.

The quality of waves is critically dependent on the quality of the winds (e.g. Durrant et al. 2013; Cardone et al. 1996; Rogers 2002), and indeed preliminary global results indicate globally averaged improvements in Significant Wave Height root-mean-square error of around 20% compared to CFSR when verified against altimeter data. Initial validation also indicates that it does not suffer from inhomogeneities through time due to changes in the assimilated observations that plagued CFSR driven wave hindcasts in the context of climate applications (e.g. Durrant et al. 2014; Chawla et al. 2012; Hemer et al. 2016).

The ERA5 wind dataset currently covers the period from 1979 to present, the same period covered by CFSR. However, this will soon be extended back to 1950, making it possible for the first time to produce wave hindcasts of 70 year duration using high-resolution consistent forcing. This increase in both quality and duration combine to provide a compelling opportunity for application in wave hindcast studies.

The Oceanum Global Wave Hindcast

Oceanum have used the ERA5 dataset to produce a global wave hindcast of unprecedented quality. The hindcast was performed with the third-generation spectral wave model WAVEWATCH III (Tolman 1991). Originally developed at the National Centers for Environmental Prediction (NCEP), WAVEWATCH III is now a widely used model with many contributors within the global scientific community (e.g Tolman et al., 2013) and has been extensively used for global and regional scale hindcasting (e.g. Chawla et al. 2012; Rascle and Ardhuin 2013; Durrant et al. 2014; Perez et al. 2017).

The Oceanum hindcast was run using the recently released version 6.07 of WAVEWATCH III. ST4 source terms were used (Ardhuin et al. 2010), which have been established over the past decade as the most suitable for global application (e.g. Stopa et al. 2015), producing significant improvements over the previous generation WAM cycle 4 terms (Bidlot et al. 2005; Janssen 1991) and Tolman and Chalikov (1996) terms (e.g. Ardhuin et al. 2010; Perrie et al. 2018). Other options include:

- The discrete interaction approximation (DIA) of Hasselmann and Hasselmann (1985) for computation of the non-linear wave-wave interactions.
- The SHOWEX bottom friction (Ardhuin et al. 2003).
- Depth-induced breaking dissipation of (Battjes and Janssen 1978) with a Miche-style shallow water limiter for maximum energy.
- Third order Ultimate Quickest propagation scheme (Leonard 1979, 1991) including the correction for spurious effects of spectral discretisation (the garden sprinkler effect), as suggested by Tolman (2002).
- Blocking of wave energy not explicitly accounted for using the subgridscale blocking approach of (Tolman 2003).

A detailed description of these model components is not provided here, and interested readers are referred to the papers listed. However, a short qualitative description of the Ardhuin et al. (2010) source terms follows. These terms consist of a modified wind input term based on (Janssen 1991), and a new dissipation term. Novel features of these terms include:

- Separate accounting of swell dissipation due to negative wind input from that due to breaking, following Tolman and Chalikov (1996).
- A non-linear swell dissipation based on observed dissipation rates across the Pacific from SAR data (Ardhuin et al. 2009)

- A breaking induced dissipation based on the local saturation spectrum rather than the total mean slope, addressing issues with the previous WAM dissipations of Komen et al. (1984).
- A cumulative dissipation rate following Young and Babanin (2006).
- A reduced wind input at high frequencies compared to Janssen (1991), and an intermediate input level at the peak, compared to the higher values with Janssen (1991), and much lower values with Tolman and Chalikov (1996). This effect is parameterised as a sheltering term, reducing the effective winds for the shorter period waves (Chen and Belcher 2000; Banner and Morison 2010).

Validation

An extensive validation of the hindcast thas been performed, both in the setup phase and of the final hindcast production run. Here we focus on validations made using altimeter data due to their global coverage, and present the annual and seasonal validation statistics. In addition, a comparison is made to a single year of the same setup forced with CFSR winds, as well as another independent state-of-the-art CFSR driven hindcast in order to quantify the relative improvement that this new hindcast offers (Figures 1 and 2). The model upgrade (physics and forcings) has resulted in significant improvements (20-30%) in wave hindcast accuracy. .

Figure 3 shows monthly hindcast statistics of H_s against all available altimeter data. In general, agreement between the altimeters and the model increases through time. This is due to improvements in the wind field with time due to increases in the number of observations assimilated and improvements in the observational accuracy with subsequent altimeter missions. Similar seasonal cycles can clearly be seen, driven primarily by seasonal differences in the Southern Ocean. Overall, validations are excellent with global biases of ±0.05 m, SI around 12-14% (with the exception of the less accurate ERS-1 and 2 altimeters), and RMS's of 0.30-0.40 m. Interannual variability is relatively small.

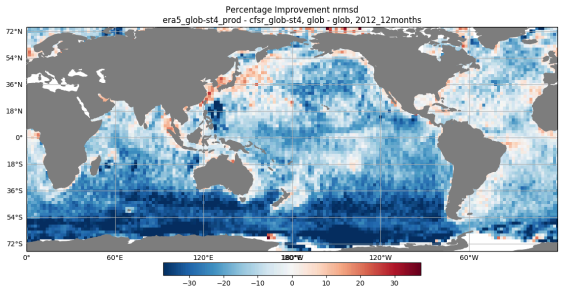

Figure 1 The percentage improvement gained with the Oceanum Global Hindcast run over previous configuration.

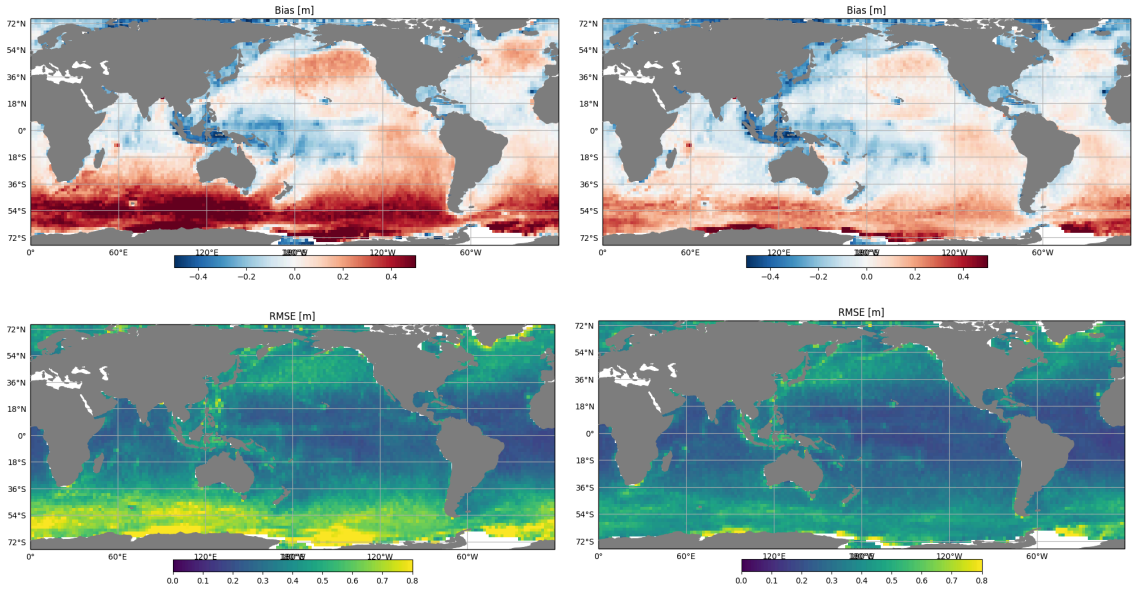

Figure 2 Bias and RMSD for CFSR winds (left plots) and ERA5 winds (right plots) in global hindcast runs.

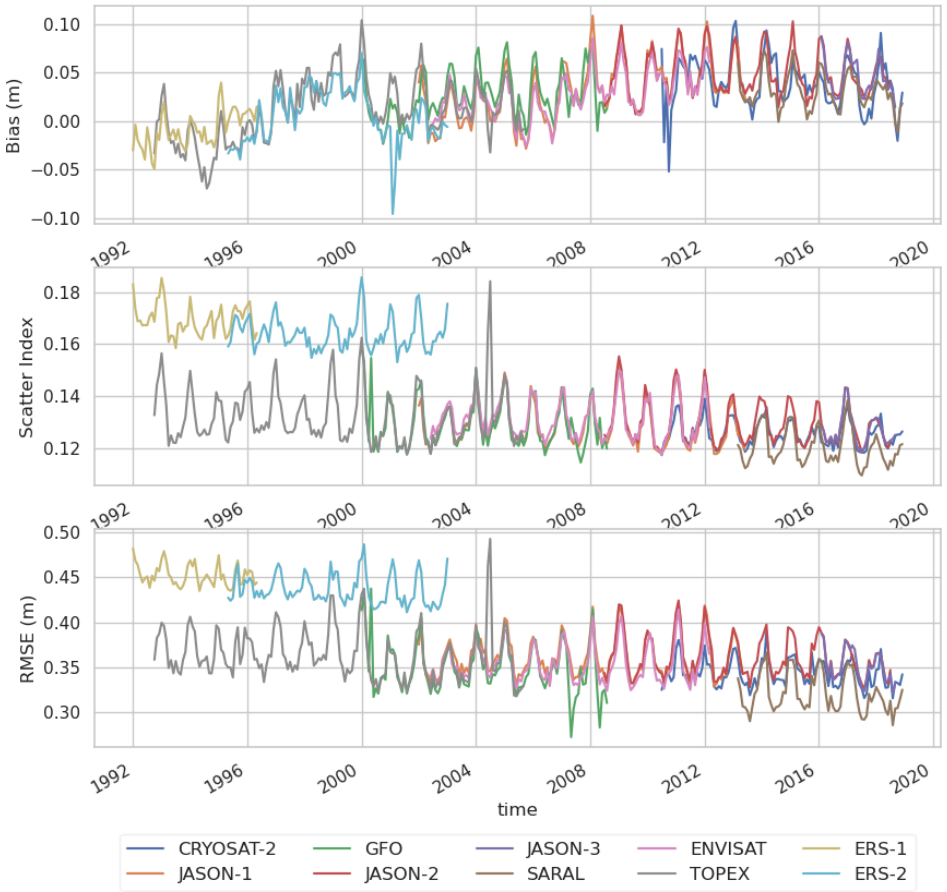

Figure 3 Time series of monthly global bias, SI, RMSD and R compared to altimeter data.

CFSR is also known to suffer from inhomogeneities through time, due to changes in the assimilated observations, to which the waves are particularly sensitive (e.g Chawla et al. 2009). Most notably, a stepwise reduction in the upper percentile winds is noted around 1993, as well as an increase in the latter years of the hindcast which can be directly seen in the wave CFSR driven hindcasts (e.g. Chawla et al. 2012; Durrant et al. 2014; Rascle and Ardhuin 2013) reducing their efficacy in climate climate applications (e.g. Hemer et al. 2016). Figure 4 shows monthly altimeter statistics of H_s for both the oceanum hindcast (same as Figure 3) and the CAWCR wave hindcast produced using CFSR wind (Durrant et. al 2014). For CFSR, the step change in 1993 is clearly evident, whereas there is no such feature present for ERA5. Similarly, the increase in bias for the last 10-15 years of the CFSR hindcast is also readily identifiable, and entirely absent from the ERA5 data. Overall, the issues associated with temporal consistency in CFSR appear to be greatly improved with ERA5. Consistent with results above, ERA5 is universally better than CFSR across the entire satellite period, with the greatest divide between the accuracy of these hindcasts occurring in the early and latter periods associated with these issues in CFSR.

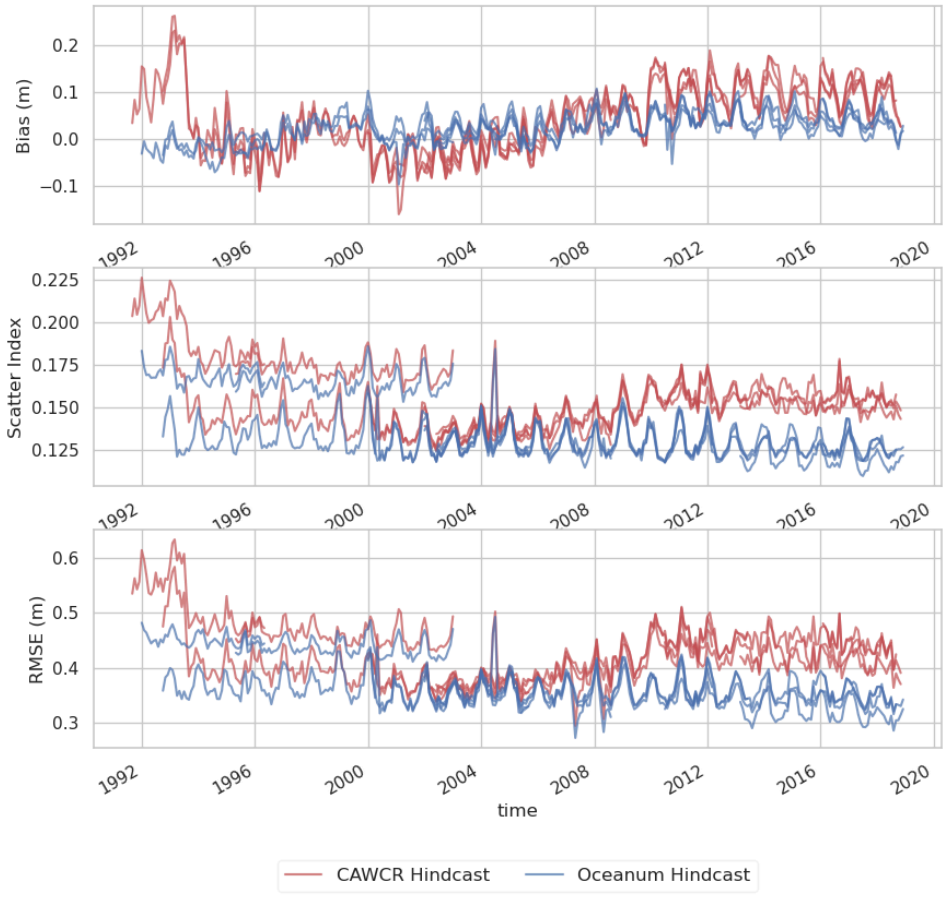

Figure 4 Times series of monthly global bias, SI, RMSD and R compared to altimeter data.

References

Ardhuin, F., T. H. C. Herbers, P. F. Jessen, and W. C. O'Reilly, 2003: Swell Transformation across the Continental Shelf. Part II: Validation of a Spectral Energy Balance Equation. *J. Phys. Oceanogr.*, **33**, 1940–1953, https://doi.org/10.1175/1520-0485(2003)033<1940:STATCS>2.0.CO;2.

——, B. Chapron, and F. Collard, 2009: Observation of swell dissipation across oceans. *Geophys. Res. Lett.*, **36**, 1–6, https://doi.org/10.1029/2008GL037030.

——, and Coauthors, 2010: Semiempirical Dissipation Source Functions for Ocean Waves. Part I: Definition, Calibration, and Validation. *J. Phys. Oceanogr.*, **40**, 1917–1941, https://doi.org/10.1175/2010JPO4324.1.

Banner, M. L., and R. P. Morison, 2010: Refined source terms in wind wave models with explicit wave breaking prediction. Part I: Model framework and validation against field data. *Ocean Model.*, **33**, 177–189, https://doi.org/10.1016/j.ocemod.2010.01.002.

Battjes, J. A., and P. A. E. M. Janssen, 1978: Energy loss and set-up due to breaking of random waves. *cedb.asce.org*, 569–587 http://cedb.asce.org/cgi/WWWdisplay.cgi?7881029.

Bidlot, J.-R., P. Janssen, and S. Abdalla, 2005: A revised formulation for ocean wave dissipation in CY29R1. *ECMWF Tech. Memo.*, **R60.9/JB/0**, 1–35.

Cardone, V. J., R. E. Jensen, D. T. Resio, V. R. Swail, and A. T. Cox, 1996: Evaluation of contemporary ocean wave models in rare extreme events: The "Halloween storm" of October 1991 and the "storm of the century" of March 1993. *J. Atmospheric Ocean. Technol.*, **13**, 198–230.

Chawla, A., D. Spindler, and H. Tolman, 2012: Validation of a thirty year wave hindcast using the climate forecast system reanalysis winds. *Ocean Model.*, https://doi.org/10.1016/j.ocemod.2012.07.005.

Chen, G., and S. E. Belcher, 2000: Effects of long waves on wind-generated waves. *J. Phys. Oceanogr.*, 2246–2256, https://doi.org/10.1175/1520-0485(2000)030<2246:EOLWOW>2.0.CO;2.

Durrant, T., D. Greenslade, M. Hemer, and C. Trenham, 2014: A Global Wave Hindcast focussed on the Central and South Pacific. *CAWCR Tech. Rep.*, **070**.

Durrant, T. H., D. J. M. Greenslade, and I. Simmonds, 2013: The effect of statistical wind corrections on global wave forecasts. *Ocean Model.*, **70**, 116–131, https://doi.org/10.1016/j.ocemod.2012.10.006.

ECMWF, 2016: *IFS Documentation CY41R2*. https://www.ecmwf.int/en/publications/ifs-documentation.

Hasselmann, S., and K. Hasselmann, 1985: *Computations and Parameterizations of the Nonlinear Energy Transfer in a Gravity-Wave Spectrum. Part I\lbrace:\rbrace A New Method for Efficient Computations of the Exact Nonlinear Transfer Integral*. 1369–1377 pp.

Hemer, M. A., S. Zieger, T. Durrant, J. O'Grady, R. K. Hoeke, K. L. McInnes, and U. Rosebrock, 2016: A revised assessment of Australia"s national wave energy resource. *Renew. Energy*, 1–23, https://doi.org/10.1016/j.renene.2016.08.039.

Janssen, P. A. E. M., 1991: Quasi-linear Theory of Wind-Wave Generation Applied to Wave Forecasting. *J. Phys. Oceanogr.*, **21**, 1631–1642.

Komen, G., S. Hasselmann, and K. Hasselmann, 1984: On the existence of a fully developed wind-sea spectrum. *J Phys Ocean.*, **14**, 1271–1285.

Leonard, B., 1979: A stable and accurate convective modelling procedure based on quadratic upstream interpolation. *Comput. Methods Appl. Mech. Eng.*, **19**, 59–98.
——, 1991: The ULTIMATE conservative difference scheme applied to unsteady one-dimensional advection. *Comput. Methods Appl. Mech. Eng.*, **88**, 17–74.
Perez, J., M. Menendez, and I. J. Losada, 2017: GOW2\lbrace:\rbrace A global wave hindcast for coastal applications. *Coast. Eng.*, **124**, 1–11, https://doi.org/10.1016/j.coastaleng.2017.03.005.
Perrie, W., and Coauthors, 2018: Modeling North Atlantic Nor'easters With Modern Wave Forecast Models. *J. Geophys. Res. Oceans*, **123**, 533–557, https://doi.org/10.1002/2017JC012868.
Rascle, N., and F. Ardhuin, 2013: A global wave parameter database for geophysical applications. Part 2: Model validation with improved source term parameterization. *Ocean Model.*, **70**, 174–188, https://doi.org/10.1016/j.ocemod.2012.12.001.
Rogers, W. E., 2002: The U.S. Navy's Global Wind-Wave Models: An Investigation into Sources of Errors in Low-Frequency Energy Predictions. *Nav. Res. Lab Tech Rep.*,.
Saha, S., and Coauthors, 2010: The NCEP Climate Forecast System Reanalysis. *Bull. Am. Meteorol. Soc.*, **91**, 1015–1057, https://doi.org/10.1175/2010BAMS3001.1.
Stopa, J. E., F. Ardhuin, A. Babanin, and S. Zieger, 2015: Comparison and validation of physical wave parameterizations in spectral wave models. *Ocean Model.*, **103**, 2–17, https://doi.org/10.1016/j.ocemod.2015.09.003.
Tolman, H. L., 1991: A Third-Generation Model for Wind Waves on Slowly Varying, Unsteady, and Inhomogeneous Depths and Currents. *J. Phys. Oceanogr.*, **21**, 782–797, https://doi.org/10.1175/1520-0485(1991)021<0782:ATGMFW>2.0.CO;2.
——, 2002: Alleviating the Garden Sprinkler Effect in wind wave models. *Ocean Model.*, **4**, 269–289.
——, 2003: Treatment of unresolved islands and ice in wind wave models. *Ocean Model.*, **5**, 219–231, https://doi.org/10.1016/S1463-5003(02)00040-9.
——, and D. V. Chalikov, 1996: Source Terms in a Third-Generation Wind Wave Model. *J. Phys. Oceanogr.*, **26**, 2497–2518.
——, M. Banner, and J. Kaihatu, 2013: The NOPP operational wave model improvement project. *Ocean Model.*, https://doi.org/10.1016/j.ocemod.2012.11.011.
Young, I., and A. Babanin, 2006: Spectral distribution of energy dissipation of wind-generated waves due to dominant wave breaking. *J. Phys. Oceanogr.*, **36**, 376–394.
Zieger, S., A. V. Babanin, W. \lbraceErick Rogers\rbrace, and I. R. Young, 2015: Observation-based source terms in the third-generation wave model WAVEWATCH. *Ocean Model.*, **96**, 2–25, https://doi.org/10.1016/j.ocemod.2015.07.014.}

Appendix A: Gridded Variables

Variable	Long Name
dir	wave mean direction
dp	peak direction
dpt	depth
fp	wave peak frequency
hs	significant height of wind and swell waves
ice	sea ice area fraction
lm	mean wave length
pdir0	wave mean direction partition 0
pdir1	wave mean direction partition 1
pdir2	wave mean direction partition 2
pdp0	peak direction partition 0
pdp1	peak direction partition 1
pdp2	peak direction partition 2
pep0	energy at peak frequency partition 0
pep1	energy at peak frequency partition 1
pep2	energy at peak frequency partition 2
pgw0	frequency width partition 0
pgw1	frequency width partition 1
pgw2	frequency width partition 2
phs0	wave significant height partition 0
phs1	wave significant height partition 1
phs2	wave significant height partition 2
plp0	peak wave length partition 0
plp1	peak wave length partition 1
plp2	peak wave length partition 2
pnr	number of wave partitions
ppe0	peak enhancement factor partition 0
ppe1	peak enhancement factor partition 1
ppe2	peak enhancement factor partition 2
pqp0	peakedness partition 0

pqp1	peakedness partition 1
pqp2	peakedness partition 2
pspr0	directional spread partition 0
pspr1	directional spread partition 1
pspr2	directional spread partition 2
psw0	spectral width partition 0
psw1	spectral width partition 1
psw2	spectral width partition 2
pt01c0	mean period T01 partition 0
pt01c1	mean period T01 partition 1
pt01c2	mean period T01 partition 2
pt02c0	mean period T02 partition 0
pt02c1	mean period T02 partition 1
pt02c2	mean period T02 partition 2
ptm10c0	mean period Tm10 partition 0
ptm10c1	mean period Tm10 partition 1
ptm10c2	mean period Tm10 partition 2
ptp0	peak period partition 0
ptp1	peak period partition 1
ptp2	peak period partition 2
pws0	wind sea fraction in partition 0
pws1	wind sea fraction in partition 1
pws2	wind sea fraction in partition 2
spr	directional spread
t01	mean period T01
t02	mean period T02
t0m1	mean period T0m1
time	julian day (UT)
tws	wind sea fraction
uuss	eastward surface stokes drift
uwnd	eastward_wind
vuss	northward surface stokes drift
vwnd	northward_wind